Time-translation-symmetry breaking in a driven oscillator:
From the quantum coherent to the incoherent regime

Yaxing Zhang,[1] J. Gosner,[2] S. M. Girvin,[1] J. Ankerhold,[2] and M. I. Dykman[3]

[1]*Department of Physics, Yale University, New Haven, Connecticut 06511, USA*
[2]*Institute for Complex Quantum Systems and IQST, Ulm University, 89069 Ulm, Germany*
[3]*Department of Physics and Astronomy, Michigan State University, East Lansing, Michigan 48824, USA*

We study the breaking of the discrete time-translation symmetry in small periodically driven quantum systems. These systems are intermediate between large closed systems and small dissipative systems, which both display such symmetry breaking but have qualitatively different dynamics. As a nontrivial example, strongly different from the familiar case of parametric resonance, we consider period tripling in a quantum nonlinear oscillator. We develop theoretical methods of the analysis of period tripling, including the theory of multiple-state resonant tunneling in phase space with the account taken of the involved geometric phase. For moderately strong driving, the period tripling persists for a time, which is exponentially long compared with all dynamical times. This time is further extended by an even weak decoherence.

I. INTRODUCTION

The breaking of translation symmetry in time, first proposed by Wilczek [1], has been attracting much attention recently. Such symmetry breaking can occur only away from thermal equilibrium [2]. It is of particular interest for periodically driven systems, which have a discrete time-translation symmetry imposed by the driving. Here, the time-symmetry breaking is manifested in the onset of oscillations with a period that is a multiple of the driving period t_F. Oscillations with period $2t_F$ due to simultaneously initialized protected boundary states were studied in photonic quantum walks [3]; period-two oscillations can also be expected from the coexistence of Floquet Majorana fermions with quasienergies 0 and $\hbar\pi/t_F$ in a cold-atom system [4]. The onset of broken time-symmetry phases was predicted and analyzed [5–10] in Floquet many-body systems, and the first observations of such phases in disordered systems were reported [11,12].

In classical systems coupled to a thermal bath, on the other hand, the effect of period doubling has been well known. A textbook example is an oscillator modulated close to twice its eigenfrequency and displaying vibrations with period $2t_F$ [13]. The oscillator has two states of such vibrations; they have opposite phases, reminiscent of a ferromagnet with two orientations of the magnetization.

The goal of this paper is to establish a relation between the symmetry breaking in the quantum coherent and incoherent regimes. Of interest in this respect are almost-isolated driven quantum systems with a few degrees of freedom. They are intermediate between large coherent systems and dissipative dynamical systems, and the transition between different regimes can be carefully examined. A driven nonlinear quantum oscillator is a good example of such an "intermediate" system. It is also of interest on its own, as it models diverse physical systems, from trapped electrons to Josephson junctions to electromagnetic and nanomechanical modes [14,15].

It follows from our analysis that an oscillator can display period doubling not only in the incoherent regime, but also in the coherent regime. However, of primary interest to us is period tripling. In a disordered system, it was observed in Ref. [12] for an elegant periodically repeated pulse sequence.

As we show, period tripling displays a number of peculiar features, which are generic for multiple-period transitions but do not occur in period doubling. They are manifested both in the presence of dissipation and in the quantum coherent regime. In a dissipative system, in contrast to period doubling (cf. Ref. [16]), the period-tripling transition cannot generically occur via the Landau-type symmetry breaking because it would require continuous merging of the symmetric (zero-amplitude) and three broken-symmetry states.

In the quantum coherent regime, period tripling reveals the nontrivial features of resonant tunneling between multiple states, which are degenerate by symmetry and are centered at points in phase space rather than coordinate space. Such tunneling is qualitatively different from the familiar resonant tunneling in a symmetric double-well potential [17] and its analysis requires new means, which we develop. We find that the tunneling is affected by a geometric phase, which comes from the discrete rotation symmetry in phase space. Combined with oscillations of the wave functions in the classically forbidden region, it results in crossing of the eigenvalues of the effective Hamiltonian with varying parameters; see Figs. 1(b) and 1(e). To make the analysis complete, we establish the conditions for the transition between the symmetry breaking in the coherent and incoherent limits.

The paper is organized as follows: In Sec. II we introduce multiple-period Floquet states of a driven oscillator, discuss the rotating wave approximation (RWA), relate the eigenvalues of the Hamiltonian in this approximation and the quasienergies, and introduce the operator of discrete rotations in phase space. In Sec. III we formulate the problem of tunneling between the minima of the RWA Hamiltonian function in phase space. In Sec. IV we calculate the symmetry-related phase difference of the intrawell functions, the geometric phase. In Sec. V we find the tunnel splitting of the lowest eigenvalues of the RWA Hamiltonian with the account taken of the oscillations of the wave functions in the classically forbidden region. In Sec. VI we discuss the onset of period tripling. We also show how dissipation leads to a transition from the coherent interwell tunneling to incoherent interwell hopping. The details of the calculations are given in Appendixes A and B. All results of
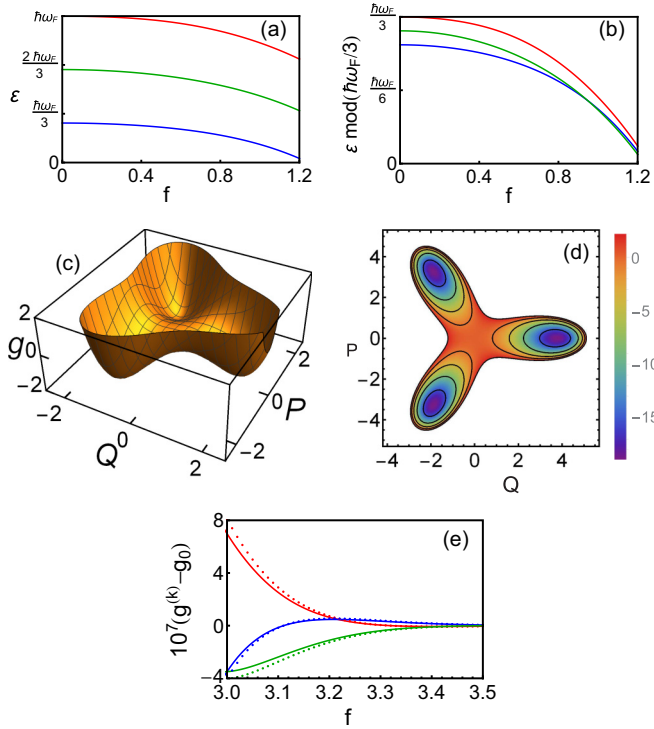
FIG. 1. (a) Quasienergy levels of a driven oscillator. The results are for the drive frequency ω_F close to $3\omega_0$, f is the scaled driving amplitude. For $f = 0$ the states from top to bottom are the lowest Fock states of the oscillator $|0\rangle$ (red), $|2\rangle$ (green), and $|1\rangle$ (blue). The same color coding is used in panels (b) and (e). The dimensionless Planck constant for motion in the rotating frame is $\lambda = 0.3$; see Eq. (8). (b) A multiplet formed when the same quasienergies are calculated mod $(\hbar\omega_F/3)$. (c) The scaled Hamiltonian function g of the driven nonlinear oscillator, Eq. (10), for $f = 1.2$; Q and P are the coordinate and momentum in the frame rotating at frequency $\omega_F/3$. (d) The orbits for several low-lying intrawell states of the Hamiltonian g for $f = 3.5$; the values of g on the orbits are in excellent agreement with the Bohr quantization condition. (e) Crossing of the scaled quasienergies $g^{(k)}$ corresponding to the tunnel-split lowest intrawell states in panel (d) and calculated mod $(\hbar\omega_F/3)$; the lowest (green), middle (blue), and top (red) curves in the range $3 < f < 3.1$ are the higher-field continuations of the middle, lowest, and top curves in panel (b) for $f < 0.4$. A superposition of the states with crossing $g^{(k)}$ is a period-three state. The dotted curves are the analytical results (19).

this paper, except for the sketches Fig. 1(d) and Fig. 3, were posted in Ref. [18].

II. MULTIPLE-PERIOD FLOQUET STATES

Coherent quantum dynamics of a driven system is conveniently described by the Floquet (quasienergy) states $\psi_\varepsilon(t)$. Such states are eigenstates of the operator T_{t_F} of time translation by t_F, $T_{t_F}\psi_\varepsilon(t) \equiv \psi_\varepsilon(t + t_F) = \exp(-i\varepsilon t_F/\hbar)\psi_\varepsilon(t)$. For a broken-symmetry state ψ_{K,ε_K} with an integer $K > 1$, time translation by t_F is not described by the factor $\exp(-i\varepsilon t_F/\hbar)$. Instead, $\psi_{K,\varepsilon_K}(t + Kt_F) = \exp(-Ki\varepsilon_K t_F/\hbar)\psi_{K,\varepsilon_K}(t)$. We call ψ_{K,ε_K} a period-K Floquet state. It is an eigenstate of $T_{Kt_F} = (T_{t_F})^K$, but not of T_{t_F}.

Multiple-period states naturally occur if the number of states of the system $\mathbb{N} \to \infty$. For such systems, the quasienergy spectrum is generally dense; cf. Ref. [19]. Then one can find states ψ_ε and $\psi_{\varepsilon'}$ with the difference of the quasienergies $|\varepsilon - \varepsilon'|$ infinitesimally close to $\hbar\omega_F/K$ with integer $K > 1$ (or to $\hbar\omega_F k/K$ with $k < K$); here $\omega_F = 2\pi/t_F$ is the driving frequency. A linear combination $\alpha\psi_\varepsilon(t) + \alpha'\psi_{\varepsilon'}(t)$ is a period-K state. The expectation values of dynamical variables in such a state oscillate with period Kt_F. However, generally the functions ψ_ε and $\psi_{\varepsilon'}$ will be of a very different form, making the oscillation amplitude exponentially small.

The situation is different for an oscillator driven close to an overtone of its eigenfrequency ω_0, i.e., for $\omega_F \approx K\omega_0$. Classically, such an oscillator in the presence of dissipation can have coexisting states of subharmonic vibrations with period $2\pi K/\omega_F$, which differ in phase by $2\pi/K$; cf. Ref. [20]. In the quantum coherent regime, the oscillator has sets of quasienergy states where the quasienergy differences within a set are very close to $\hbar\omega_F/K$ in a broad parameter range. These states result from tunnel splitting of the states symmetrically positioned in phase space and localized near the minima (or maxima) of the Hamiltonian function of the oscillator in the frame rotating at frequency ω_F/K; see Figs. 1(c) and 1(d).

As we show below, for some interrelations between the parameters, for pairs of the localized symmetric states in phase space the tunnel splitting becomes exactly zero. Respectively, in the laboratory frame the quasienergy difference between such states is exactly equal to $\hbar\omega_F/K$. Off-diagonal matrix elements of the dynamical variables calculated for the corresponding states are large, making a linear combination of the states a directly observable coherent period-K state of the oscillator.

In a way, for a parametric oscillator ($K = 2$) the occurrence of a coherent period-two state could be inferred from the results [21] where vanishing of the tunnel splitting was found. However, this state was not identified there and the time-symmetry breaking was not addressed. Sets of states separated by $\approx\hbar\omega_F/K$ were found numerically for $K \gg 1$ for a special model of an oscillator in the interesting paper [22]; the considered states did not break time symmetry. Tunnel splitting in phase space was carefully studied for modulated cold-atom systems; cf. Refs. [23,24] and references therein. Recently it was also found numerically for such systems for states with period π/ω_F [25]; in contrast to the work reported in Refs. [3–10], the results of Ref. [25] do not describe quantum-coherent breaking of time-translation symmetry.

The rotating wave approximation and the rotation operators in phase space

We study a most commonly used model of a nonlinear oscillator, the Duffing model, which describes a broad range of the systems mentioned in the Introduction [14,15,26]. Its Hamiltonian reads

$$H = H_0 + H_F, \quad H_0 = \tfrac{1}{2}p^2 + \tfrac{1}{2}\omega_0^2 q^2 + \tfrac{1}{4}\gamma q^4, \quad (1)$$

where q and p are the oscillator coordinate and momentum. The term $H_F \equiv H_F(t)$ describes the driving. In the analysis of parametric resonance, one chooses $H_F = -\tfrac{1}{2}q^2 F \cos\omega_F t$

with $\omega_F \approx 2\omega_0$. Here we consider

$$H_F = -\tfrac{1}{3}q^3 F \cos\omega_F t, \quad \omega_F \approx 3\omega_0.$$

Our results apply also for additive driving $H_F = -qF'\cos\omega_F t$, if one replaces $F \to 3\gamma F'/8\omega_0^2$; this relation may be useful for an experimental implementation of period tripling.

If the driving is not too strong, so that the expectation values of H_F, γq^4, and $\omega_F(\omega_F - K\omega_0)q^2$ are small compared with the expectation value of $\omega_0^2 q^2$, the oscillator dynamics can be described in the rotating wave approximation (RWA) [27]. For an oscillator driven close to the Kth overtone of its eigenfrequency, one makes a canonical transformation $U(t) = \exp(-ia^\dagger a\omega_F t/K)$, where a and $a^\dagger$ are the ladder operators, $[a,a^\dagger] = 1$. The RWA Hamiltonian H_{RWA} is obtained by time averaging the transformed Hamiltonian $\tilde{H}(t) = U^\dagger(t)H(t)U(t) - i\hbar U^\dagger(t)\dot{U}(t)$,

$$H_{\text{RWA}} = (Kt_F)^{-1}\int_0^{Kt_F} dt\,\tilde{H}(t). \tag{2}$$

Clearly, H_{RWA} is independent of time.

1. Relating quasienergies to the eigenvalues of H_{RWA}

If $\phi(t)$ is an eigenfunction of H_{RWA}, i.e., $H_{\text{RWA}}\phi = E\phi$, then the corresponding wave function in the laboratory frame is $\psi(t) = U(t)\phi(t)$, and

$$T_{t_F}\psi(t) = e^{-iEt_F/\hbar}U(t+t_F)\phi(t) = e^{-iEt_F/\hbar}N_K\psi(t). \tag{3}$$

We call E the RWA energy. The operator N_K introduced in Eq. (3) is

$$N_K = \exp(-2\pi i a^\dagger a/K), \quad [N_K, H_{\text{RWA}}] = 0. \tag{4}$$

The relation $[N_K, H_{\text{RWA}}] = 0$ follows from the expression $\tilde{H}(t+t_F) \equiv N_K^\dagger \tilde{H}(t)N_K$ for the transformed (but not period-averaged) Hamiltonian combined with Eq. (2). It was obtained in Ref. [22] for a specific form of H_{RWA}.

Operators N_K^k with $k = 0,1,\ldots,K-1$ form a cyclic group. Then the eigenfunctions $\phi^{(k)}$ of N_K are

$$N_K\phi^{(k)} = \exp(-2\pi i k/K)\phi^{(k)}, \quad 0 \leqslant k \leqslant K-1. \tag{5}$$

Functions $\phi^{(k)}$ are also eigenfunctions of H_{RWA}. From Eqs. (3) and (5), a wave function $\phi^{(k)}$ with RWA energy $E^{(k)}$ corresponds to a Floquet state with quasienergy

$$\varepsilon^{(k)} = (E^{(k)} + \hbar\omega_F k/K)\text{mod}(\hbar\omega_F). \tag{6}$$

As we will see, for sufficiently strong drive the eigenstates of H_{RWA} form multiplets with close eigenvalues $E^{(k)}$. The quasienergies of different states in the multiplets differ by $\approx \hbar\omega_F/K$.

Equation (5) allows one to write the functions $\phi^{(k)}$ in terms of the Fock states of the oscillator $|n\rangle$. These states are eigenstates of the operator $a^\dagger a$, $a^\dagger a|n\rangle = n|n\rangle$. From Eq. (5), only one out of each K Fock states contributes to $\phi^{(k)}$,

$$\phi^{(k)} = \sum_n C_n^{(k)}|Kn+k\rangle.$$

This relation significantly simplifies numerical diagonalization of H_{RWA}, as the coefficients $C_n^{(k)}$ with different k are uncoupled. Most importantly, it shows that the RWA energy levels of states

with different k can *cross* when the parameters of the system vary. This crossing is seen in Fig. 1. In contrast, the RWA energies of states with the same k *avoid crossing*.

2. Rotating-wave-approximation Hamiltonian for period tripling

We now consider the explicit form of H_{RWA} for our system. The oscillator motion in the rotating frame is conveniently described by the coordinate Q and momentum P, which are related to q and p as

$$U^\dagger(t)[q + i(K/\omega_F)p]U(t) = C(Q+iP)e^{-i\omega_F t/K}. \tag{7}$$

The parameter C is the scaling factor that makes Q and P dimensionless,

$$[Q,P] = i\lambda, \quad \lambda = \frac{\hbar K}{\omega_F C^2}, \quad a = \frac{Q+iP}{\sqrt{2\lambda}}. \tag{8}$$

The dimensionless Planck constant λ and the parameter C for $K = 2$ are given in Ref. [28]. For period tripling ($K = 3$), $C = (8\omega_F\delta\omega/9\gamma)^{1/2}$, where $\delta\omega = \tfrac{1}{3}\omega_F - \omega_0$ is the frequency detuning from the resonance, $|\delta\omega| \ll \omega_F$. This scaling is convenient for $\gamma\,\delta\omega > 0$; the opposite case will be considered elsewhere. In what follows, for convenience we assume $\delta\omega, \gamma > 0$.

It is immediately seen from Eqs. (4) and (8) that N_K are rotation operators in the (Q,P) plane:

$$N_K^\dagger Q N_K = Q\cos(2\pi/K) + P\sin(2\pi/K),$$
$$N_K^\dagger P N_K = -Q\sin(2\pi/K) + P\cos(2\pi/K). \tag{9}$$

For the chosen scaling, the Hamiltonian H_{RWA} has the form $H_{\text{RWA}} = [8\omega_F^2(\delta\omega)^2/27\gamma]\hat{g}(Q, -i\lambda\partial_Q)$ with

$$g(Q,P) = \tfrac{1}{4}(Q^2 + P^2 - 1)^2 - \tfrac{1}{3}f(Q^3 - 3PQP), \tag{10}$$

where $f = F/(8\omega_F\gamma\delta\omega)^{1/2}$ is the scaled amplitude of the driving. Function $g(Q,P)$ is shown in Fig. 1(c). This function is the dimensionless Hamiltonian function in the rotating frame. It has three minima, three saddle points, and a local maximum at $Q = P = 0$.

III. MULTIWELL TUNNELING IN PHASE SPACE

Period tripling provides a platform for studying generic features of tunneling between degenerate states centered at points located in phase space. As seen from Fig. 1(c), function $g(Q,P)$ has a threefold rotational symmetry in the (Q,P) plane. This symmetry follows from Eqs. (4) and (9), since N_3 is an operator of rotation by the angle $-2\pi/3$ in phase plane.

The minima of $g(Q,P)$ lie at the vertices (Q_m,P_m) of an equilateral triangle; we count $m = 0,1,2$ counterclockwise and set $m = 0$ for the vertex with $P_0 = 0$; the enumeration implies that the states $m = -1$ and $m = 2$ are the same. The values of Q_m, P_m are given in Appendix A. For not too weak driving, the three lowest eigenstates of the operator $\hat{g} \equiv g(Q, -i\lambda\partial_Q)$ are tunnel-split superpositions of the three lowest degenerate intrawell states in Fig. 1(d). We denote these intrawell states by Ψ_m ($m = 0,1,2$).

One can think of a function Ψ_m as an eigenfunction of the operator $\hat{g}_m$, which approximates operator $\hat{g}$ for Q close to Q_m and P close to P_m. In particular, in its central part Ψ_m is

an eigenfunction of the operator $\hat{g}$ expanded to second order in $Q - Q_m$, $P - P_m$. Then $\hat{g}_m \Psi_m = g_0 \Psi_m$; the eigenvalue g_0 is the same for all wells by symmetry. In the explicit form g_0 is given by Eq. (A3). From Eq. (9), $N_3^\dagger \hat{g}_m N_3 = \hat{g}_{m+1}$. This is because rotation of Q, P by the angle $-2\pi/3$ in Eq. (9) is equivalent to rotation of Q_m, P_m by the angle $2\pi/3$. Then $\hat{g}_{m-1} N_3 \Psi_m = N_3 (N_3^\dagger \hat{g}_{m-1} N_3) \Psi_m = N_3 \hat{g}_m \Psi_m = g_0 N_3 \Psi_m$, and thus $N_3 \Psi_m$ is the eigenfunction of the operator $\hat{g}_{m-1}$, which shows that $N_3 \Psi_m = \Psi_{m-1}$.

If our system is in a state Ψ_m and the tunneling can be disregarded, the time symmetry is broken. Indeed, from Eqs. (3), (7), and (9), time translation by t_F transforms

$$\Psi_m \rightarrow N_3 \Psi_m = \Psi_{m-1}. \quad (11)$$

From Eq. (11), to come back to state Ψ_m, one has to increment time by $3t_F$. The relation $\Psi_{m+1} = N_3^\dagger \Psi_m$ gives the phase shift between functions Ψ_{m+1} and Ψ_m. Since N_3 is a rotation operator, this phase shift is geometric in nature (see below).

Since (i) the minima of the effective Hamiltonian $\hat{g}$ are located in phase space, not in the coordinate space, and (ii) there are three equal-depth minima, resonant tunneling between states Ψ_m differs from the familiar tunneling in a symmetric double-well potential [17]. To find the tunnel splitting of the lowest eigenvalues of $\hat{g}$, we write the wave functions Ψ_m in the coordinate representation, $\Psi_m \equiv \Psi_m(Q)$. The three normalized eigenstates $\phi^{(k)}$ of $\hat{g}$ with the smallest eigenvalues $g^{(k)}$ ($k = 0, 1, 2$) have the standard form of the tight-binding theory

$$\phi^{(k)}(Q) = \frac{1}{\sqrt{3(1 + \delta^{(k)})}} \sum_{m=0,1,2} \Psi_m(Q) e^{-2mk\pi i/3}, \quad (12)$$

where $\delta^{(k)} = 2\text{Re}[\langle \Psi_0 | \Psi_1 \rangle \exp(-2\pi i k/3)] \ll 1$. We choose $\Psi_0(Q)$ to be real and normalized. Since $\Psi_{m+1} = N_3^\dagger \Psi_m$, we have $\Psi_2(Q) = \Psi_1^*(Q)$. Due to the symmetry, the functions $\phi^{(k)}$ can be shown to be orthogonal.

The wave functions Ψ_m are Gaussian near the corresponding extrema of $g(Q, P)$ in phase space; see Appendix A and Eqs. (A4) and (A15) below. However, to find the tunnel splitting it is necessary to find the tails of Ψ_m in the classically inaccessible regions. In solving this problem one has to take into account that the effective Hamiltonian $\hat{g}$ is not quadratic in the momentum P.

We calculate the eigenvalues $g^{(k)}$ by using the relation

$$\int_\infty^{Q_*} dQ [\phi^{(k)}(Q)(\hat{g} - g_0)\Psi_0(Q)$$
$$- \Psi_0(Q)(\hat{g} - g^{(k)})\phi^{(k)}(Q)] = 0, \quad (13)$$

with g_0 being the value of $\hat{g}$ in the lowest intrawell state in the neglect of tunneling [cf. Fig. 1(d)], $g_0 \approx \min g(Q, P) + \lambda \omega_{\min}/2$, where $\omega_{\min}$ is the eigenfrequency of vibrations about a minimum of $g(Q, P)$, which is determined by the curvature of $g(Q, P)$ near the minimum; the explicit values of g_0, Q_m, P_m, and $\omega_{\min}$ are given by Eqs. (A1) and (A2). The difference $g^{(k)} - g_0$ is exponentially small for a small dimensionless Planck constant λ.

An important distinction from the standard analysis of resonant tunneling [17] is that the upper limit Q_* of the integral (13) is not known in advance. This is because the Hamiltonian

$\hat{g}$ does not have the symmetry $Q \rightarrow -Q$ of the standard symmetric double-well potential [17]. To choose Q_* we note that the functions $\Psi_m(Q)$ fall off exponentially away from their respective maxima Q_m. Thus, Ψ_0 and $\Psi_{1,2}$ fall off in the opposite directions in the classically forbidden region between Q_0 and Q_1. We choose Q_* within this region in such a way that $\Psi_{0,1,2}(Q_*)$ are all of the same order of magnitude. The integral (13) should be independent of Q_*.

The Wenzel–Kramers–Brillouin (WKB) expressions for the wave functions $\Psi_{0,1}(Q)$ in the region between Q_1 and Q_0 are given in Appendix A,

$$\Psi_m(Q) = C_m (i\partial_P g)^{-1/2} e^{iS_m(Q)/\lambda} \quad (m = 0, 1),$$
$$\partial_Q S_m = (-1)^m \tilde{P}(Q), \quad g(Q, \tilde{P}) = g_0. \quad (14)$$

Here, $S_m(Q)$ is the classical action and $\tilde{P}(Q)$ is the classical momentum given by equation $g(Q, \tilde{P}) = g_0$; we choose the branch $\text{Im}\tilde{P} < 0$ with the smallest $|\text{Im}\tilde{P}|$. It is critical that, because the Hamiltonian function $g(Q, P)$ is quartic in P, $\tilde{P}(Q)$ has a branch point Q_B given by Eq. (A8), which lies deep in the interval (Q_1, Q_0) where $\text{Im}\tilde{P} \neq 0$. For $Q_1 < Q < Q_B$, $\tilde{P}(Q)$ has both imaginary and real parts. The positions of the minima and Q_B are shown in Appendix A in Fig. 3.

The real part of the action $S_m(Q)$ in the classically inaccessible region leads to oscillations of the wave functions in this region. These oscillations lie behind the crossing of the levels $g^{(k)}$ calculated with the account taken of the interwell tunneling.

IV. THE GEOMETRIC PHASE

The normalization constants C_m in Eq. (14) are determined by the wave functions inside the wells, where the functions are large. If we choose Ψ_0 real, the parameter C_0 is fixed. The rotation symmetry (11) shows that $\Psi_1 = N_3^\dagger \Psi_0$, and therefore the parameters C_0 and C_1 are not independent. The relation between them is determined by a phase θ_1. This phase can be found using the explicit Gaussian form of the intrawell wave functions obtained in Appendix A. To make the reading easier, we give them here, too, and include the explicit expression for the prefactor of Ψ_1,

$$\Psi_0(Q) = (\sqrt{\pi} l_q)^{-1/2} \exp[-(Q - Q_0)^2/2l_q^2], \quad (15)$$

$[l_q = [\lambda \omega_{\min}/(Q_0^2 + 1)]^{1/2}]$, and

$$\Psi_1(Q) = C_{1,\text{intra}} \exp[(iP_1(Q - Q_1) - \tfrac{1}{2}\varkappa_1(Q - Q_1)^2)/\lambda],$$
$$C_{1,\text{intra}} = [\text{Re}\varkappa_1/\pi\lambda]^{1/4} \exp(i\theta_1). \quad (16)$$

We note that the Gaussian-width parameter in Ψ_1 is complex valued, $\varkappa_1 = [2\omega_{\min} + i\sqrt{3}(fQ_0 - 1)]/3Q_0^2$. The prefactor $C_{1,\text{intra}}$ contains the geometric phase θ_1. This prefactor is written in the form which is consistent with the form of the Gaussian distribution (A15), except for the unknown at this time phase θ_1. The "intrawell" normalization factor $C_{1,\text{intra}}$ differs from the coefficient C_1 that determines the behavior of the function Ψ_1 on its tail in the classically inaccessible region.

To calculate θ_1, we introduce an auxiliary coherent state $|\alpha\rangle$ and consider the overlap integral of this state with the wave functions $\Psi_{0,1}$. By construction $a|\alpha\rangle = \alpha|\alpha\rangle$, and thus $N_3|\alpha\rangle = |\alpha \exp(-2\pi i/3)\rangle$ [we recall that

$N_3 = \exp(-2\pi i a^\dagger a/3)$]. By using that $\Psi_0 = N_3\Psi_1$, we obtain a formal relation $\langle\alpha|\Psi_0\rangle = \langle\alpha\exp(2\pi i/3)|\Psi_1\rangle$. If we now choose the state $|\alpha\rangle$ in such a way that it strongly overlaps with Ψ_0, whereas $|\alpha\exp(2\pi i/3)\rangle$ strongly overlaps with Ψ_1, this relation will allow us to find θ_1 by calculating the corresponding overlap integrals using the explicit expressions (15) and (16). Writing $|\alpha\rangle$ in the coordinate representation as

$$|\alpha\rangle = \frac{1}{(\pi\lambda)^{1/4}} \exp\left\{-\frac{1}{2}(|\alpha|^2 - \alpha^2) - \frac{[Q - (2\lambda)^{1/2}\alpha]^2}{2\lambda}\right\}$$

and setting $\alpha = Q_0/\sqrt{2\lambda}$, we obtain

$$\theta_1 = \tfrac{1}{2}\arg(\varkappa_1 + 1) + P_1 Q_1/2\lambda. \tag{17}$$

The geometric phase θ_1 has a large term $\propto\lambda^{-1}$. It also contains a term independent of λ, which must be kept, because it determines the phase of the oscillations of the wave function in the classically forbidden region.

V. LEVEL SPLITTING

The explicit expressions for the wave functions $\Psi_m(Q)$ allow us to calculate the level splitting by using Eq. (13). For Q_* well inside the interval (Q_1, Q_0), we have $\int_\infty^{Q_*}\Psi_0^2(Q)dQ = -1$. Taking into account that overlapping of the functions $\Psi_{1,2}(Q)$ with $\Psi_0(Q)$ is exponentially small, we rewrite Eq. (13) as

$$g^{(k)} - g_0 \approx \left[\int_\infty^{Q_*} dQ\,\Psi_1(Q)\hat{g}\Psi_0 - \int_\infty^{Q_*} dQ\,\Psi_0\hat{g}\Psi_1(Q)\right]$$
$$\times \exp(-2k\pi i/3) + \text{c.c.} \tag{18}$$

It is important that the product $\Psi_0(Q)\Psi_1(Q)$ has two terms. One of them is $\propto\exp\{i[S_0(Q) + S_1(Q)]/\lambda\}$. It depends smoothly on Q, because $S_0(Q) + S_1(Q) = \text{const.}$ for $Q_1 < Q < Q_0$; cf. Eq. (14). The other term is $\propto\exp\{-i[S_0^*(Q) - S_1(Q)]/\lambda\}$, it is a fast oscillating function of Q. The contribution of this term to the integrals (18) is exponentially small and exponentially sensitive to the change of Q_* on the scale $\propto\lambda$. Therefore this term should be disregarded.

Calculating the integrals in Eq. (18) by parts, carefully accounting for the branching of $\tilde{P}(Q)$, and using Eq. (14) we find that Q_* indeed drops out from the expression for the level splitting. The result is Eq. (B1). It gives the splitting in terms of the complex classical momentum $\tilde{P}(Q)$ calculated for the scaled energy $g(Q, \tilde{P}) = \min g + \lambda\omega_{\min}/2$. It is convenient to express the splitting in terms of the momentum that does not contain the effective Planck constant λ. The corresponding transformation is discussed in Appendix B. The result reads

$$g^{(k)} - g_0 = C_{\text{tun}} e^{-S_{\text{tun}}/\lambda} \cos(\lambda^{-1}\Phi_{\text{tun}} - 2\pi k/3). \tag{19}$$

In contrast to the tunnel splitting in a symmetric double-well potential [17], the splitting (19) has not only an exponential, but also an oscillating factor. The tunneling exponent S_{tun} and the tunneling phase Φ_{tun} are given by the expression

$$\Phi_{\text{tun}} + i S_{\text{tun}} = \int_{Q_0}^{Q_1} dQ'\,P_{\text{cl}}(Q') + \lambda K_{\text{tun}} + \lambda\theta_1. \tag{20}$$

Here, P_{cl} is the momentum on the instanton trajectory that goes from the $m = 0$ to the $m = 2$ minimum of $g(Q, P)$; $g(Q, P_{\text{cl}}) = \min g$, $\text{Re}\,P_{\text{cl}} < 0$, and $\text{Im}\,P_{\text{cl}} < 0$.
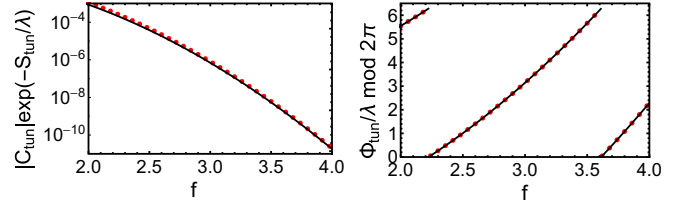

FIG. 2. (left panel) The amplitude of the tunnel splitting of the scaled RWA energy levels, which is given by Eq. (19) without the oscillating factor. (right panel) The phase of the tunnel splitting. Black solid lines show the results of the numerical solution of the eigenvalue problem for the Hamiltonian $g(Q, -i\lambda\partial_Q)$. Red dotted lines show Eq. (19). The results refer to $\lambda = 0.3$.

Parameter K_{tun} gives terms $O(\lambda)$ in the arguments of the exponent and the cosine in Eq. (19). The calculation in Appendix B shows that

$$K_{\text{tun}} = \int_{Q_0}^{Q_B} dQ\,k(Q, Q_0) + \int_{Q_B}^{Q_1} dQ\,k(Q, Q_1), \tag{21}$$

where $k(Q, Q_m) = [\omega_{\min}(\partial_P g)_{\text{cl}}^{-1} - i|Q - Q_m|^{-1}]/2$ [the subscript "cl" indicates that the derivative is calculated for $P = P_{\text{cl}}$; the explicit expression for $k(Q, Q_m)$ is given in Eq. (B2)]. Equation (21) is free from divergences. We note that $\text{Im}\,K_{\text{tun}}$ can be considered as a part of the prefactor, but $\text{Re}\,K_{\text{tun}}$ gives a shift of the phase of the level splitting and therefore is very important for determining the parameter values where the quasienergies of different states differ exactly by $\hbar\omega_F/3$; see below.

Because of the branching of the momentum on the instanton trajectory, the prefactor in Eq. (19) has a more complicated form than for tunneling in a double-well potential [29]. However, it is also $\propto\hbar^{1/2}$; explicitly, $C_{\text{tun}} = -2\lambda^{3/4}\omega_{\min}[(Q_B - Q_1)(Q_0 - Q_B)\sqrt{\text{Re}\,\varkappa_1}/\pi l_q]^{1/2}$.

The explicit expression (19) is in extremely good agreement with the numerical results obtained by solving the Schrödinger equation $g(Q, -i\lambda\partial_Q)\phi^{(k)} = g^{(k)}\phi^{(k)}$. This can be seen from Fig. 1(e). Both the numerical values of the amplitude of the splitting and the phase agree with the analytical results; see Fig. 2. Equation (19) simplifies in the limit of comparatively strong drive, $f \gg 1$. The leading-order terms in S_{tun} and in Φ_{tun} are quadratic in f. Numerically, the asymptotic regime is reached for comparatively large f, where the tunneling amplitude becomes very small.

VI. PERIOD TRIPLING

Equation (19) is *the central result of this paper*. It shows that the splitting of the eigenvalues of H_{RWA} oscillates as the system parameters vary. Two eigenvalues cross each time $\lambda^{-1}\Phi_{\text{tun}} = (n + n'/3)\pi$ with integer n and $n' = 0, 1, 2$. Such crossings are seen in Figs. 1(b) and 1(e). Given that the RWA energy $E^{(k)} \propto g^{(k)}$, it follows from Eqs. (3) and (5) that an oscillator in a superposition of states with equal $g^{(k)}$ displays period tripling. Similarly, when in the case of a parametric oscillator the quasienergy difference is exactly $\hbar\omega_F/2$ [21,30], a superposition of the corresponding states is a period-two state.

From the explicit expression (19), period tripling occurs in a broad range of the field amplitudes and frequencies. Importantly, the level crossing is robust with respect to the terms disregarded in the RWA. Such terms can only lead to a small shift of the crossing points.

Where the eigenvalues $g^{(k)}$ do not cross, they stay exponentially close to each other. Respectively, the quasienergy difference is exponentially close to $\hbar\omega_F/3$ on the scale $\hbar\delta\omega$ or $\hbar F^2/\omega_F\sqrt{|\gamma|}$. Similar triples of states result from the tunnel splitting of the excited intrawell states in Fig. 1(d).

For the oscillator in a superposition of states $\phi^{(k)}$ and $\phi^{(k')}$ with $g^{(k)} \neq g^{(k')}$, the expectation values of the variables still have period $3t_F$, if measured over time smaller than the exponentially long time $|\Omega_{kk'}|^{-1}$, where $\Omega_{kk'} = \lambda^{-1}[g^{(k)} - g^{(k')}]\delta\omega, |\Omega_{kk'}/\delta\omega| \ll 1$. The Fourier spectra of the expectation values have components at frequencies $|(k - k')\omega_F/3 + \Omega_{kk'}|$. If the driven oscillator has charge, it can radiate; the radiation spectrum displays a peak shifted from $\omega_F/3$ by $|\Omega_{kk'}|$.

As seen from Fig. 1(b), a superposition of states $\phi^{(k)}$ and $\phi^{(k')}$ with close $g^{(k)}$ and $g^{(k')}$ can be prepared by ramping up the driving field, if initially the oscillator is in a superposition of Fock states $|n\rangle$ and $|n'\rangle$ with $|n - n'|(\text{mod}3) \neq 0$. There is no threshold in the field amplitude F for preparing a multiple-period state: by varying the frequency detuning of the field $\delta\omega$ one can obtain such a state for an arbitrarily small F. Moreover, starting from a judiciously prepared linear combination of the three lowest Fock states of the oscillator, one can prepare the system in any of the lowest intrawell states. Similarly, it actually follows from the results of Ref. [30] that there should be no threshold for preparing period-two states of an oscillator parametrically driven at close to twice its eigenfrequency.

From coherent to dissipative period tripling

Even weak dissipation of the oscillator can qualitatively change its dynamics. It breaks the coherence of the intrawell states Ψ_m. If the dissipation rate Γ exceeds the exponentially small frequencies $|\Omega_{kk'}|$, instead of coherent resonant tunneling between the wells of $g(Q, P)$, the oscillator performs incoherent interwell hopping, the process analogous to the well-known quantum diffusion. Phenomenologically, by symmetry arguments, the hopping is described by the balance equation for the state populations ρ_{mm},

$$\dot{\rho}_{mm} = W \sum_{m' \neq m} \rho_{m'm'} - 2W\rho_{mm}.$$

Since the intrawell states are the broken-symmetry states of period-three vibrations that differ only in phase, hopping corresponds to a slip of the vibration phase by $2\pi/3$. On times small compared with the reciprocal hopping rate W^{-1} the oscillator stays in an intrawell state. This is the exact analog of the classical behavior where, as is well known for a parametric oscillator, the multiple-period state is seen on times short compared with the reciprocal rate of interstate switching. We emphasize that, for a longer observation time, all coexisting states are seen and there is no time-symmetry breaking.

The rate W is exponentially sensitive to the system parameters. In the standard quantum diffusion theory ρ_{mm} is the diagonal matrix element of the density matrix ρ on functions Ψ_m and $W \propto \Omega_{kk'}^2/\Gamma$, where one should use the

maximum value of $|\Omega_{kk'}|$; clearly, $W \ll |\Omega_{kk'}| \ll \Gamma$ [31,32]. However, the actual situation for a driven oscillator is more complicated.

The full analysis of interwell hopping should take into account dissipation-induced transitions to the excited intrawell states, which occur even for $T = 0$ [15]. The rate of interwell transitions in highly excited states is high. However, their population is exponentially small. As a result, the condition $W \ll \Gamma$ holds. The balance equation in this case describes the evolution of the well populations rather than the populations of the lowest states in the wells and should be modified to include transitions to the zero-amplitude state. The analysis of this process is beyond the scope of this paper.

For a small decay rate Γ, a quantum oscillator initially in the ground state can be brought into the intrawell states by adiabatically ramping up the field to reach small $|\Omega_{kk'}| \ll \Gamma$ and then waiting for a time longer than Γ^{-1}. The intrawell states will be equally populated. However, repeated measurements separated by $\delta t \ll W^{-1}$ will show the oscillator in the same state, a signature of the broken time symmetry. In contrast, and this is an important feature of period tripling, a classical oscillator would stay in the zero-amplitude state when the field is ramped up, because the classical driving force is $\propto q^2 F$; the zero-amplitude state does not merge with broken-symmetry states for $K > 2$, in contrast to the parametric oscillator.

VII. CONCLUDING REMARKS

A promising type of oscillators for observing period tripling is modes of microwave cavities coupled to Josephson junctions. Recently there have been studied systems where inelastic Cooper pair tunneling leads to an effective driving of a cavity mode that depends nonlinearly on the mode coordinate and has a tunable frequency $2eV/\hbar$ determined by the voltage V across the Josephson junction [33–35]. There are also other possibilities to resonantly excite multiple-period modes in microwave cavities [36].

In conclusion, we studied a quantum oscillator driven close to an overtone of its eigenfrequency and showed that such a small quantum system can display coherent multiple-period dynamics. Relaxation with the rate exceeding the exponentially small tunnel splitting breaks the coherence. The system can then be observed in one of the broken-symmetry states, which are localized in phase space and have a lifetime exponentially longer than the relaxation time. Studying the previously unexplored case of period tripling allowed us to develop a general approach to finding the tunnel splitting for systems with multiple degenerate states and to revealing and evaluating the geometric phase between multiple degenerate states in phase space. It also demonstrated the qualitative difference between the transitions to multiple-period states in the coherent and dissipative regimes. The results fill in the gap between the topologically protected broken-symmetry Floquet states in extended systems and multiple-period states in dissipative systems.

APPENDIX A: THE INTRAWELL WAVE FUNCTIONS OF THE ROTATING-WAVE-APPROXIMATION HAMILTONIAN

The scaled Hamiltonian function $g(Q,P)$ of the driven oscillator in the rotating wave approximation (RWA) is given by Eq. (10) and is plotted in Fig. 1(c). It has three symmetrically located minima at points (Q_m, P_m) with $m = 0,1,2$ (see Fig. 3),

$$Q_0 = \tfrac{1}{2}[f + (f^2 + 4)^{1/2}], \quad Q_1 = Q_2 = -Q_0/2,$$
$$P_0 = 0, \quad P_1 = -P_2 = \sqrt{3}Q_0/2. \tag{A1}$$

From the explicit form of the function $g(Q,P)$ we find the minimal value of this function $g_{\min}$ and the dimensionless frequency of classical vibrations about a minimum $\omega_{\min} = \{\det[\partial^2_{x_i x_j} g(x_1, x_2)]\}^{1/2}$ (the derivatives are calculated at a minimum of g),

$$g_{\min} = -\tfrac{1}{12}f Q_0(Q_0^2 + 3), \quad \omega_{\min} = [3f Q_0(Q_0^2 + 1)]^{1/2}. \tag{A2}$$

The frequency $\omega_{\min}$ is the same for all minima, and so is the lowest eigenvalue g_0 of the Hamiltonian $\hat{g}(Q, -i\lambda\partial_Q)$ in the neglect of tunneling. To the lowest order in the dimensionless Planck constant λ it corresponds to the lowest eigenvalue of a harmonic oscillator with frequency $\omega_{\min}$,

$$g_0 = g_{\min} + \tfrac{1}{2}\lambda\omega_{\min}. \tag{A3}$$

1. The wave function $\Psi_0(Q)$

Near the minimum (Q_0, P_0) we have $g(Q,P) \approx g_{\min} + \tfrac{1}{2}(Q_0^2 + 1)(Q - Q_0)^2 + \tfrac{3}{2}f Q_0 P^2$. The wave function $\Psi_0(Q)$ is Gaussian for $|Q - Q_0| \ll |Q_1 - Q_0|$ and can be chosen to be real,

$$\Psi_0(Q) = (\sqrt{\pi} l_q)^{-1/2} \exp\left[-(Q - Q_0)^2/2l_q^2\right], \tag{A4}$$

with $l_q = [\lambda\omega_{\min}/(Q_0^2 + 1)]^{1/2}$ being the localization length.

We are interested in the tail of Ψ_0 for Q between the minima of $g(Q,P)$, i.e., for $Q_1 < Q < Q_0 - l_q$. The WKB form of $\Psi_0(Q)$ is given by Eq. (14) of the main text, which we here write explicitly,

$$\Psi_0(Q) = C_0(i\partial_P g)^{-1/2} \exp[iS_0(Q)/\lambda],$$
$$S_0(Q) = \int_{Q_0 - l_q}^{Q} dQ' \tilde{P}(Q'), \tag{A5}$$

with $\tilde{P}(Q)$ given by equation $g(Q, \tilde{P}) = g_0$ and $\partial_P g$ calculated for $P = \tilde{P}(Q)$.

For the branch of $\tilde{P}$ that we are interested in,

$$\tilde{P}(Q)^2 = A(Q) + B^{1/2}(Q), \quad A(Q) = 1 - Q^2 - 2f Q,$$
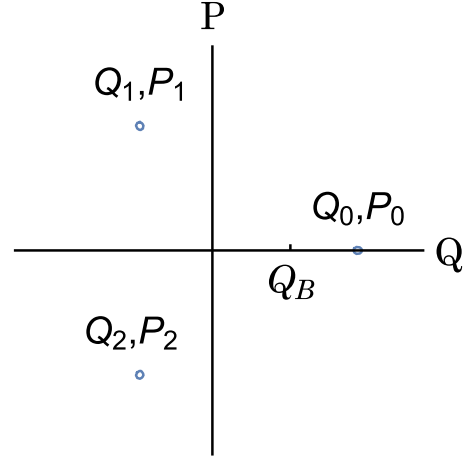$$B(Q) = A^2(Q) - 4[g(Q,0) - g_0], \tag{A6}$$

FIG. 3. Positions of the minima (Q_m, P_m) ($m = 0,1,2$) of the function $g(Q,P)$ and of the branching point Q_B. The wave function $\Psi_0(Q)$ monotonically decays away from Q_0 in the region $Q > Q_B$, whereas in the region $Q_1 < Q < Q_B$ the decay is accompanied by oscillations.

with $\mathrm{Im}\tilde{P} < 0$ for $Q < Q_0$; we keep the correction $\propto \lambda$ to secure matching to Eq. (A4).

For Q close to Q_0 and $Q < Q_0 - l_q$, we have $A(Q) < 0$, $B(Q) > 0$, and $A(Q) + B^{1/2}(Q) < 0$. Therefore $\tilde{P}(Q)$ is purely imaginary and the same is true for the function

$$\partial_P g = \tilde{P}(Q)B^{1/2}(Q), \tag{A7}$$

with $i\partial_P g > 0$. Accordingly, $\Psi_0(Q)$ exponentially decays with increasing $Q_0 - Q$. The prefactor C_0 is determined by matching Eqs. (A4) and (A5) for Q close to Q_0 but $Q_0 - Q \gg l_q$,

$$C_0 = (\omega_{\min}/2\sqrt{\pi e})^{1/2}.$$

As Q decreases, first $B(Q)$ becomes equal to zero at point Q_B; see Fig. 3. To leading order in $\lambda \ll 1$

$$Q_B \approx Q_0 - \tfrac{3}{4}f. \tag{A8}$$

For still smaller Q, $A(Q)$ changes sign to positive. This happens for $Q_B > Q > Q_1 \equiv -Q_0/2$. Importantly,

$$A(Q_1) = P_1^2 > 0, \quad B(Q_1) = 2\lambda\omega_{\min}. \tag{A9}$$

In the explicit form, the imaginary part of the momentum in the classically forbidden region is

$$\mathrm{Im}\tilde{P}(Q) = -\left[-A(Q) - B^{1/2}(Q)\right]^{1/2} \quad (Q_B < Q < Q_0),$$
$$\mathrm{Im}\tilde{P}(Q) = -\left[(A^2 + |B|)^{1/2} - A\right]^{1/2}/\sqrt{2} \quad (Q < Q_B). \tag{A10}$$

As discussed in the main text, the level splitting crucially depends on the oscillations of the wave function under the barrier. These oscillations start with the decreasing Q at $Q = Q_B$. Near Q_B we have $B(Q) \approx \partial_Q B(Q_B)(Q - Q_B)$, whereas $A(Q_B) < 0$. Therefore $\tilde{P} \approx -i|A(Q_B)|^{1/2} + (i/2)|\partial_Q B(Q_B)/A(Q_B)|^{1/2}(Q - Q_B)^{1/2}$ for small $Q - Q_B > 0$, i.e., Q_B is a branching point of $\tilde{P}(Q)$. Going around this

point in the complex plane [17], we find that, for $Q < Q_B$,

$$\Psi_0(Q) \approx 2C_0 |\partial_P g|^{-1/2} \exp\left[-\text{Im}S_0(Q)/\lambda\right] \cos \Phi_0(Q),$$
$$\Phi_0(Q) = \Phi_0'(Q) + \Phi_0''(Q). \tag{A11}$$

Here, the phase $\Phi_0'(Q)$ comes from the real part of the action,

$$\Phi_0'(Q) = \lambda^{-1} \int_{Q_B}^{Q} dQ' \text{Re}\tilde{P}(Q'),$$
$$\text{Re}\tilde{P}(Q) = -[(A^2 + |B|)^{1/2} + A]^{1/2}/\sqrt{2}, \tag{A12}$$

whereas $\Phi_0''(Q)$ comes from the prefactor, with account taken of going around Q_B in the complex plane,

$$\Phi_0''(Q) = -\frac{1}{2} \arcsin[\text{Re}\tilde{P}(Q)/|\tilde{P}(Q)|] - \frac{\pi}{4}. \tag{A13}$$

The choice of $\text{Re}\tilde{P}$ and $\text{Im}\tilde{P}$ in Eqs. (A10) and (A12) corresponds to writing $B^{1/2} = i|B|^{1/2}$ in Eq. (A6) for $\tilde{P}^2$ in the region where $B(Q) < 0$.

The WKB approximation (A5) breaks down near Q_1, as $B(Q)$ becomes $\sim\lambda$ and $|\partial_P g|$ becomes small. However, we do not need to calculate the wave function $\Psi_0(Q)$ in this region, as seen from Eq. (13).

2. The wave function $\Psi_1(Q)$

The minimum of $g(Q,P)$ at (Q_1,P_1) corresponds to a nonzero momentum $P_1 > 0$. Therefore the wave function Ψ_1 centered at Q_1 is complex valued even near its maximum. Calculating Ψ_1 involves three steps: finding it inside the well of $g(Q,P)$ near Q_1, P_1; finding the geometric phase, that relates Ψ_1 and Ψ_0 given that Ψ_0 is chosen in the form (A4), and then finding the tail of Ψ_1 in the classically forbidden range.

a. The intrawell wave function

Using the explicit form (A1) of Q_1, P_1, to the second order in $\delta Q = Q - Q_1$, $\delta P = P - P_1$ we write the Hamiltonian near (Q_1, P_1) as

$$g(Q,P) \approx g_{\min} + \tfrac{3}{4}(1 + fQ_0)\delta P^2 + \tfrac{1}{4}(1 + 5fQ_0)\delta Q^2$$
$$+ (\sqrt{3}/4)(fQ_0 - 1)[\delta Q \delta P + \text{H.c.}]. \tag{A14}$$

The expression for Ψ_1 for $|\delta Q| \ll Q_0 - Q_1$ then reads

$$\Psi_1(Q) = C_{1,\text{intra}} \exp\left[\left(iP_1\delta Q - \tfrac{1}{2}\varkappa_1 \delta Q^2\right)/\lambda\right],$$
$$\varkappa_1 = [2\omega_{\min} + i\sqrt{3}(fQ_0 - 1)]/3Q_0^2. \tag{A15}$$

The Gaussian-width parameter $\varkappa_1$ is now complex valued, and so is the prefactor $C_{1,\text{intra}}$, which has a phase factor $\exp(i\theta_1)$. This phase is calculated in the main text.

b. The wave function Ψ_1 in the classically forbidden region

In the case of the wave function Ψ_1, Eq. (14) for the wave function in the classically forbidden region reads

$$\Psi_1(Q) = C_1(i\partial_P g)^{-1/2} \exp[iS_1(Q)/\lambda], \tag{A16}$$

$$S_1(Q) = -\int_{Q_1+l_q'}^{Q} dQ' \tilde{P}(Q'),$$

where $\tilde{P}(Q)$ is given by Eqs. (A10) and (A12), $l_q' = [\lambda/\text{Re}\varkappa_1]^{1/2}$. Equation (A16) corresponds to choosing $B^{1/2}(Q) = i|B(Q)|^{1/2}$ for $B(Q) < 0$ and to $\partial_P g$ calculated for $P(Q) = \tilde{P}(Q)$, i.e., $\partial_P g = \tilde{P}B^{1/2}$. For $Q_B - Q \gg Q - Q_1 \gg l_q'$ we have $-\tilde{P}(Q) \approx P_1 + i\varkappa_1(Q - Q_1)$, as expected from Eq. (A15). By matching Eqs. (A15) and (A16), we find

$$C_1 = (\omega_{\min}/2\sqrt{\pi e})^{1/2} \exp(i\theta_1'),$$
$$\theta_1' = \theta_1 - \lambda^{-1}\left[\left(l_q'^2/2\right)\text{Im}\varkappa_1 - P_1 l_q'\right]. \tag{A17}$$

Because we count the action S_1 off from $Q_1 + l_q'$, there emerges an extra phase factor in C_1 due to the oscillations of the wave function inside the "potential well" centered at (Q_1, P_1).

APPENDIX B: TUNNEL SPLITTING OF THE SCALED ROTATING-WAVE-APPROXIMATION ENERGY LEVELS

Using the explicit form of the operator $g(Q, -i\lambda\partial_Q)$ we obtain from Eq. (18)

$$g^{(k)} - g_0 = -2\lambda C_0 |C_1| \exp(-S_\lambda/\lambda) \cos\left(\frac{\Phi_\lambda}{\lambda} - \frac{2k\pi}{3}\right),$$

$$S_\lambda = -\int_{Q_1+l_q'}^{Q_0-l_q} dQ \,\text{Im}\tilde{P}(Q),$$

$$\Phi_\lambda^{(k)} = -\int_{Q_1+l_q'}^{Q_B} dQ \,\text{Re}\tilde{P}(Q) + \lambda\theta_1'. \tag{B1}$$

This expression is somewhat inconvenient, because $\tilde{P}$ is calculated with account taken of the term $\propto \lambda$. It is easy to see that $\tilde{P}(Q) \approx P_{\text{cl}}(Q) + \frac{1}{2}\lambda\omega_{\min}/\partial_P g$, where P_{cl} is given by the value of the classical momentum calculated for $\lambda = 0$. This approximation breaks down near Q_0, Q_B, and Q_1 where $\partial_P g$ goes to zero. Similar to Ref. [29], for $Q_0 > Q > Q_B$ one can write

$$\int_{Q_0-l_q}^{Q} dQ' \tilde{P}(Q') \approx \int_{Q_0}^{Q} dQ' [P_{\text{cl}}(Q') + \lambda k(Q', Q_0)]$$
$$- \frac{i\lambda}{2} \ln \frac{|Q - Q_0|}{l_q} - \frac{i\lambda}{4} - \frac{i\lambda}{2} \ln 2,$$

$$k(Q, Q_m) = \frac{\omega_{\min}}{2P_{\text{cl}}(Q)B_{\text{cl}}^{1/2}(Q)} - \frac{i}{2|Q - Q_m|}. \tag{B2}$$

Here, $B_{\text{cl}}(Q) = (16f/3)(Q - Q_1)^2(Q - Q_B)$ is the value of $B(Q)$ calculated for $\lambda = 0$. A similar transformation can be made for $\int_{Q_1+l_q'}^{Q} dQ' \tilde{P}(Q')$ in the region $Q_1 < Q < Q_B$.

We now have to consider the vicinity of Q_B. Formally, the quantum correction to $P_{\text{cl}}(Q)$ diverges at Q_B. However, the divergence is integrable. Therefore Eq. (B2) applies all the way until $Q = Q_B$, and one can use the value of Q_B given by Eq. (A8).

The final result for the difference of the scaled RWA energies is Eq. (19) of the main text.

[1] F. Wilczek, Phys. Rev. Lett. **109**, 160401 (2012).

[2] H. Watanabe and M. Oshikawa, Phys. Rev. Lett. **114**, 251603 (2015).

[3] T. Kitagawa, M. A. Broome, A. Fedrizzi, M. S. Rudner, E. Berg, I. Kassal, A. Aspuru-Guzik, E. Demler, and A. G. White, Nat. Commun. **3**, 882 (2012).

[4] L. Jiang, T. Kitagawa, J. Alicea, A. R. Akhmerov, D. Pekker, G. Refael, J. I. Cirac, E. Demler, M. D. Lukin, and P. Zoller, Phys. Rev. Lett. **106**, 220402 (2011).

[5] A. Chandran and S. L. Sondhi, Phys. Rev. B **93**, 174305 (2016).

[6] V. Khemani, A. Lazarides, R. Moessner, and S. L. Sondhi, Phys. Rev. Lett. **116**, 250401 (2016).

[7] C. W. von Keyserlingk and S. L. Sondhi, Phys. Rev. B **93**, 245146 (2016).

[8] D. V. Else, B. Bauer, and C. Nayak, Phys. Rev. Lett. **117**, 090402 (2016).

[9] N. Y. Yao, A. C. Potter, I.-D. Potirniche, and A. Vishwanath, Phys. Rev. Lett. **118**, 030401 (2017).

[10] V. Khemani, C. W. von Keyserlingk, and S. L. Sondhi, Phys. Rev. B **96**, 115127 (2017).

[11] J. Zhang, P. W. Hess, A. Kyprianidis, P. Becker, A. Lee, J. Smith, G. Pagano, I.-D. Potirniche, A. C. Potter, A. Vishwanath, N. Y. Yao, and C. Monroe, Nature (London) **543**, 217 (2017).

[12] S. Choi, J. Choi, R. Landig, G. Kucsko, H. Zhou, J. Isoya, F. Jelezko, S. Onoda, H. Sumiya, V. Khemani, C. von Keyserlingk, N. Y. Yao, E. Demler, and M. D. Lukin, Nature (London) **543**, 221 (2017).

[13] L. D. Landau and E. M. Lifshitz, *Mechanics*, 3rd ed. (Elsevier, Amsterdam, 2004).

[14] J. Tan and G. Gabrielse, Phys. Rev. Lett. **67**, 3090 (1991).

[15] M. I. Dykman (ed.), *Fluctuating Nonlinear Oscillators: from Nanomechanics to Quantum Superconducting Circuits* (Oxford University Press, Oxford, 2012).

[16] Z. R. Lin, Y. Nakamura, and M. I. Dykman, Phys. Rev. E **92**, 022105 (2015).

[17] L. D. Landau and E. M. Lifshitz, *Quantum Mechanics. Non-Relativistic Theory*, 3rd ed. (Butterworth-Heinemann, Oxford, 1997).

[18] Y. Zhang, J. Gosner, S. M. Girvin, J. Ankerhold, and M. Dykman, arXiv:1702.07931.

[19] D. W. Hone, R. Ketzmerick, and W. Kohn, Phys. Rev. A **56**, 4045 (1997).

[20] A. H. Nayfeh and D. T. Mook, *Nonlinear Oscillations* (Wiley-VCH, Weinheim, 2004).

[21] M. Marthaler and M. I. Dykman, Phys. Rev. A **76**, 010102(R) (2007).

[22] L. Guo, M. Marthaler, and G. Schön, Phys. Rev. Lett. **111**, 205303 (2013).

[23] W. K. Hensinger, H. Haffer, A. Browaeys, N. R. Heckenberg, K. Helmerson, C. McKenzie, G. J. Milburn, W. D. Phillips, S. L. Rolston, H. Rubinsztein-Dunlop, and B. Upcroft, Nature (London) **412**, 52 (2001).

[24] D. A. Steck, W. H. Oskay, and M. G. Raizen, Science **293**, 274 (2001).

[25] K. Sacha, Phys. Rev. A **91**, 033617 (2015).

[26] V. Peano and M. Thorwart, Chem. Phys. **322**, 135 (2006).

[27] D. F. Walls and G. J. Milburn, *Quantum Optics* (Springer, Berlin, 2008).

[28] M. Marthaler and M. I. Dykman, Phys. Rev. A **73**, 042108 (2006).

[29] A. Garg, Am. J. Phys. **68**, 430 (2000).

[30] Y. Zhang and M. I. Dykman, Phys. Rev. A **95**, 053841 (2017).

[31] Y. Kagan, J. Low Temp. Phys. **87**, 525 (1992).

[32] M. I. Dykman and G. G. Tarasov, Zh. Eksp. Teor. Fiz. **74**, 1061 (1978) [Sov. Phys. JETP **47**, 557 (1978)].

[33] M. Hofheinz, F. Portier, Q. Baudouin, P. Joyez, D. Vion, P. Bertet, P. Roche, and D. Esteve, Phys. Rev. Lett. **106**, 217005 (2011).

[34] A. D. Armour, M. P. Blencowe, E. Brahimi, and A. J. Rimberg, Phys. Rev. Lett. **111**, 247001 (2013).

[35] V. Gramich, B. Kubala, S. Rohrer, and J. Ankerhold, Phys. Rev. Lett. **111**, 247002 (2013).

[36] P. Delsing, D. Esteve, and F. Portier (private communication).